International Journal of Civil Engineering and Infrastructure
Vol. 2, No. 1, March 2022

EVALUATING THE PERCEPTION OF STRUCTURAL DEFECTS DURING IMPLEMENTATION OF RC T-BEAMS

EL-Said A. Bayoumi[1,2]
[1]Department of Civil Engineering, College of Engineering, Qassim University, Buraidah, Saudi Arabia
[2]Engineering Expert at Ministry of Justice, Egypt
Correspondence email: saidbay80@hotmail.com

Received December 03, 2021 | Accepted February 10, 2022

ABSTRACT

Most defects during construction projects are due to human errors which happen due to poor workmanship. This study involved 8 simply supported RC T-beams subjected to uniformly distributed load at both-edges of slab. The investigated parameters were the effect of malposition of slab reinforcement, unequal configuration of slab reinforcement and change in bar diameter of slab reinforcement. The experimental results showed that; malposition of slab reinforcement leads to a lower load carrying capacity of the slab and consequently flexural resistance decreased and slab deflection increased. The irregularity of the reinforcing bars in concrete slab affected the load carrying capacity of T-beam. Well-arranged distribution of reinforcement improves the ductile behavior of slab and reduced value of deflections at failure. Using reinforcing steel bars with diameters higher than 8mm in the reinforcement helped the slab to withstand more loads. The use of 10mm diameter in reinforcement of the slab enhances the serviceability of T-beams.

Keywords*: Human errors; Construction defects; malposition; unequal configuration; T-beam*

1. INTRODUCTION

There are many projects are being implemented all over the world. Some of the projects involve the construction of buildings. Nevertheless, some of the buildings are poorly constructed and maintained. The concrete structure needs to be inspected and maintained regularly. In the last few years, a number of concrete buildings collapsed in the world under apparent normal circumstances. These failures are pre-dominantly due to human errors within the design or during construction of these buildings. Cracks in concrete may affect appearance only or may indicate significant structural distress or a lack of durability. Cracks may represent the total extent of the damage or may point to problems of greater magnitude. Their significance depends on the type of structure, as well as the nature of cracking [1-2].

Few investigations have addressed the shortcomings which frequently existed in the execution and cracking in reinforced concrete (RC) structures. These defects can be classified into two main categories; the

first category focuses on the defects that occur in the detailing of reinforcing bars and cracking in RC elements, while the other category focuses on the compressive strength of concrete [3-5].

In Egypt, Housing and Building National Research Center (HBNRC) has conducted a statistical study on the causes of deterioration in concrete structures in various periods. This statistical study illustrated that about 83% of the causes of damage were referred to bad execution practices starting from the eighties of the past century. Thus, there is an increasing demand for developing a better understanding of the effect of bad execution practices on the performance of concrete structures, especially on cracking in order to determine the proper method of repairing these defects [6-7].

Reinforced concrete (RC) structures consist of a series of members. The flooring of buildings have a slab-beam system, in which the slab spans between beams, which in turn applies loads to columns and the column loads are applied to footings, which distribute the load over a sufficient area of soil. Most of the reinforced concrete systems are cast monolithic. During construction, concrete from the bottom of the deepest beam to the top of slab, is placed at once. Therefore the slab serves as the top flange of the beams. The concrete slabs and beams act together in resisting the applied loads. As a result, the beam will have an extension concrete part at the top called flange and the portion of the beam below the slab is called the web. To consider a slab and a beam as a T-section, it is necessary to ensure interaction between these elements by a solid connection. Connection in the contact between the slab and the beam must be capable of ensuring a proper resistance to longitudinal and transverse flexural forces. T-section beams with the advantages of easy construction and saving costs have been extensively used in the design of flooring systems and are still in use as an economic and efficient construction system [8-9].

An experimental study was carried out to investigate the serviceability behavior of normal strength concrete (NSC) and high strength concrete (HSC) T-beams by I. Shaaban et al. They studied the effect of flange dimensions (breadth and thickness) on the crack pattern. It was found that an increase in the flange dimensions (breadth and thickness) delayed the cracks initiation, its propagation and increased the maximum applied load prior to failure, and reduced the short term deflection of the beams. Prior to failure, the increment in the maximum loads was up to 22% while the deflection reduced by 31% for NSC and 23% for HSC beams [10].

R. Thamrin et al. [11] investigated shear strength of reinforced concrete T-beams without stirrups. The test variables were type of beam cross section and ratio of longitudinal reinforcement. Six simply supported beams, consisting of three beams with rectangular cross section and three beams with T-section beams, subjected to two point load were tested until failure. They concluded that shear capacity of T-beams were higher for rectangular beams, with the values ranging from 5 to 25%, depending on the ratio of longitudinal reinforcement which influences the shear capacity of the beam as well as the angle of diagonal shear crack.

A number of researchers conducted studies on the shear strength behavior of the reinforced concrete T-beams. They found that; an increase in the ratio of flange width to web width is shown to produce an accompanying increase in the ultimate strength of a reinforced concrete T-beam, provided the ratio of flange depth to an effective depth is above a particular minimum value. The existence of slab contributed to increase the shear resistance in the T-beams, where the shear failure loads increase by 42% of rectangular section in the T-beams without stirrups

and ratio up to 43% in the T-beams with ordinary web stirrups while the ratio up to 54% in the T-beams with flange stirrups. The shear resistance increases with the increase of slab thickness. When the ratio of slab thickness to beam thickness increase from 13% to 27% the shear failure loads increases by ratio 45%. Increases in the flange width of a T-beam give higher shear capacity with a nonlinear relationship for the T-beam with shear reinforcement [12-15].

M. Słowik [16] studied an experimental study to discuss the failure in T-beams with various reinforcement ratio. In case of higher reinforced concrete T-beams without transverse reinforcement, he found that; a shear failure which is caused by the growth of diagonal cracks whereas, a brittle failure due to the formation of a flexural crack takes place in case of plain and slightly reinforced concrete T-beams. The maximum permissible load was depended on concrete crushing in the compression zone or steel yielding.

An investigation of the compression flange in T-beam sections (change of dimensioning the width to the web of T-beam) under concentrated loads effect was studied. They were concluded that; the existence of the compression flange in T-beams improved the shear capacity load with respect to equivalent rectangular cross sections. The failure in T-beam without shear reinforcement was exhibited an inclined cracks were noted starting from its upper side of the flange (where the inclined shear crack continued as a diagonal crack in the flange) to support points [17-20].

2. EXPERIMENTAL PROGRAM

The experimental program consisted of constructing and testing of 8 simply supported T- beams, where specimens were loaded on the slab only with uniformly distributed load at both edges of slab, as shown in **Fig. 1.**

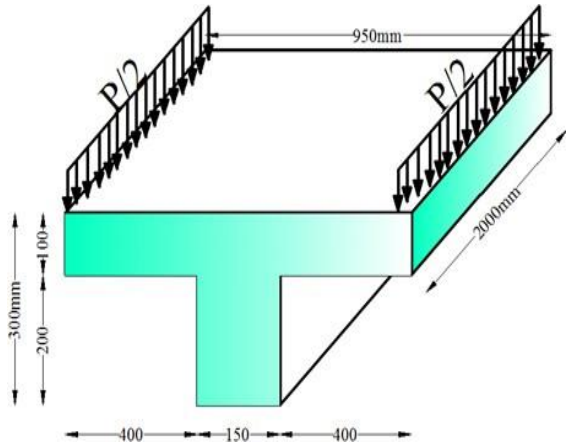

Figure 1. Two-uniform distributed line loads at both edges of the slab

The dimensions of T-beam specimens used in this investigation were 150mm×200mm×2000mm in web-width, depth and length, respectively. The thickness and width of the flange of the T- section beams are 100mm and 950mm, respectively. **Table 1** show the details of specimens.

Table 1. Details of the T-beam specimens

Group	Specimen ID	Notes
Malposition of slab reinforcement (GIM)	GIM-1 (Control)	($t_{mis.}/t_s$) ×100 = 20%
	GIM-2	($t_{mis.}/t_s$) ×100 = 40%
	GIM-3	($t_{mis.}/t_s$) ×100 = 60%
	GIM-4	($t_{mis.}/t_s$) ×100 = 80%
Effect of unequal configuration of slab reinforcement (GIIA)	GIIA-1	———
	GIIA-2	———
Effect of change in bar diameter of slab reinforcement (GIIID)	GIIID-1	Slab reinforcement = 11Ø6/m
	GIIID-2	Slab reinforcement = 4Ø10/m

Details of Specimens

All the T-section beams were simply supported with a clear span of 1800mm. Two types of steel reinforcement were used in fabricating T-beam sections. Reinforcement of the flange (slab) and the stirrups of the projected beam (web) were mild-steel (yield strength of 240MPa), and all the projected beams were reinforced with 3Ø10 bars as a main (bottom) and a secondary (top) reinforcement (high-grade steel with yield strength of 360MPa). The modulus of elasticity for steel reinforcement was considered asEs=210GPa.

The vertical stirrups reinforcement was 8mm diameter spaced at 200mm acting as transverse reinforcement. The reinforcement of the slab was changed from specimen to specimen according to the type of parameter. **Fig. 2** shows the dimensions and geometry of the control specimen

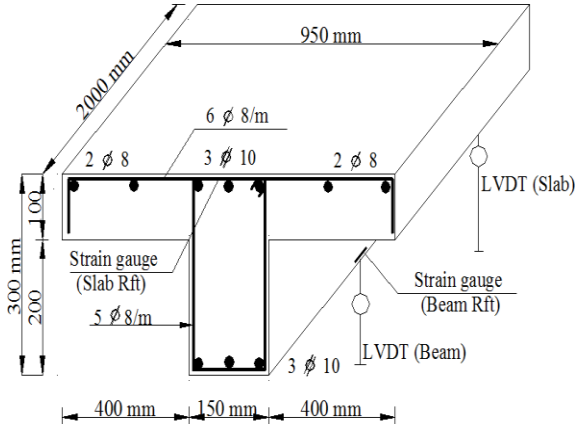

Figure 2. Details of control specimen

Details of Experimental Parameters

The specimens were subjected to uniform distributed loads at both-ends of slab and were divided into three parameters. The first parameter discussed the impact of malposition of slab reinforcement, the second parameter investigated the effect of unequal configuration of slab reinforcement while the last parameter examined the effect of a change in bar diameter of slab reinforcement on the efficiency of whole T-beam sections.

The first parameter consisted of four specimens, GIM-1 (control), GIM-2, GIM-3, and GIM-4, as shown in **Fig. 3**. The variable of all these specimens was the depth of slab reinforcement. The malposition of slab reinforcement was ($t_{mis.}/t_s$) varied as 20%, 40%, 60% and 80%, respectively where $t_{mis.}$ is the misplacement of slab reinforcement while t_s is the thickness of slab. Control specimen (GIM-1) was made with standard requirements of good compaction using a

mechanical vibrator, enough concrete cover, well- arranged reinforcement. No splices in the reinforcement of slab or beam were used in this control specimen. All specimens were constructed in the laboratory at Faculty of Engineering, AL-Azhar University.

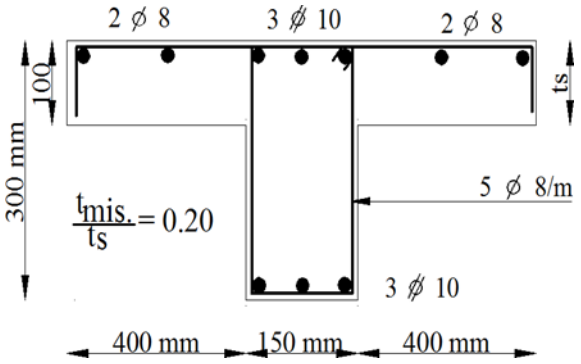

Figure 3 (a). Details of specimen GIM-1

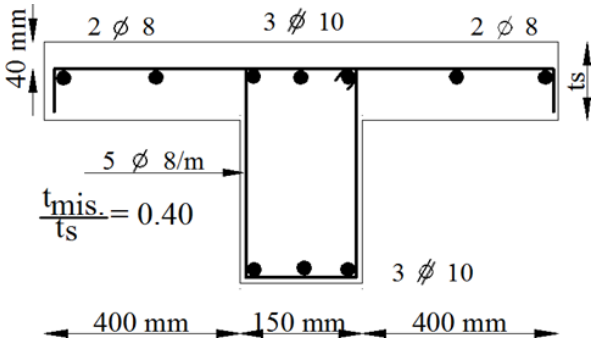

Figure 3 (b). Details of specimen GIM-2

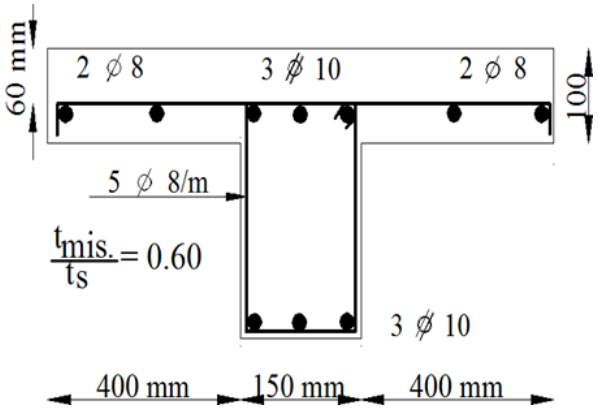

Figure 3 (c). Details of specimen GIM-3

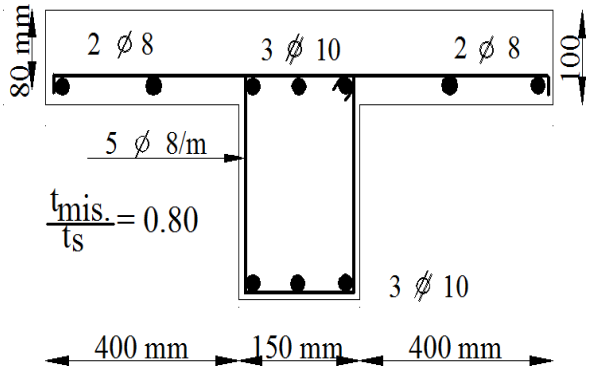

Figure 3 (d). Details of specimen GIM-4

While the second parameter contained two specimens, in addition to the control specimen. In this group, eccentricity of the main steel in slab was the major parameter. The area of steel for slab was constant (13Ø8mm on the length of the slab), but the distribution of steel was varied for two specimens (unequal distribution of slab reinforcement). In first specimen GIIA-1, unequal arrangement of slab reinforcement was used with three reinforcement bars at the mid-span of the slab at 50mm while two bars were placed at the distance of 260mm from two sides from the previous three bars keeping the distance between these bars as 50mm. Moreover, there are two bars from two sides at the distance of 260mm from the end of the slab. At the ends of the specimen one bar was erected. In another specimen GIIA-2, the eccentricity of slab reinforcement was in three groups, every group comprises three bars, and there are two distances between three bars. This distance was 100mm while the distance between groups was 290mm. At the end of the specimen, two bars were erected from two sides, and the distance was 100mm. Plan of slab reinforcement distribution for specimen GIIA-2.

Figure 4 illustrates plan of reinforcement distribution of slab specimen GIIA-1 and GIIA-2.

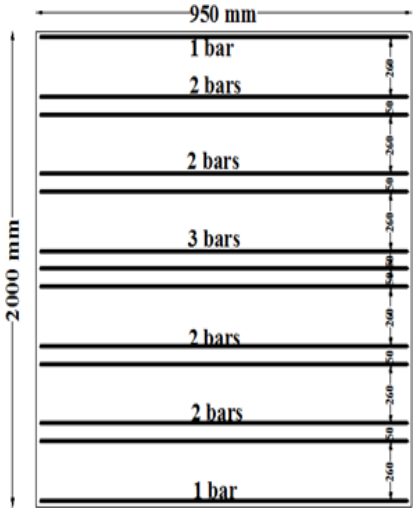

Figure 4 (a). Plan of specimen GIIA-1

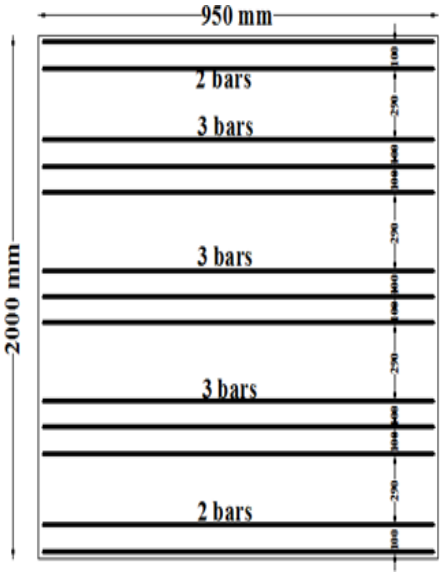

Figure 4 (b). Plan of specimen GIIA-2

The last parameter comprised of three specimens GIIID-1, GIIID-2, in addition to the control specimen GIM-1, and identifies the change in bar diameter of slab reinforcement, as shown in **Fig. 5**. The ratio of steel was not changed but the diameter only was changed. The first specimen was of the diameter 6mm (mid steel) whereas the diameter of 10mm (high-tensile steel) was used in the second specimen. In the first specimen GIIID-1, the area of steel was fulfilled by 11Ø6/m while the second specimen GIIID-2 comprise 4Ø10/m.

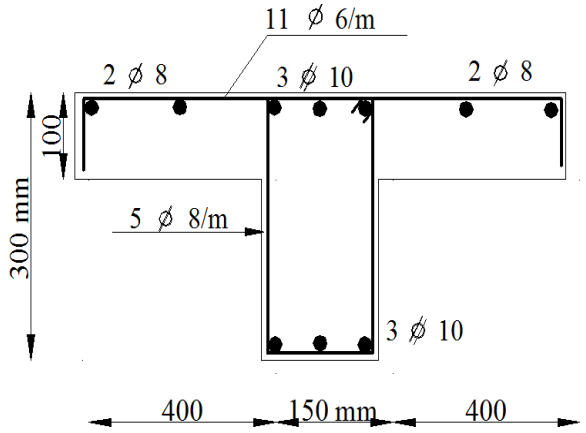

Figure 5 (a). Plan of specimen GIIID-1

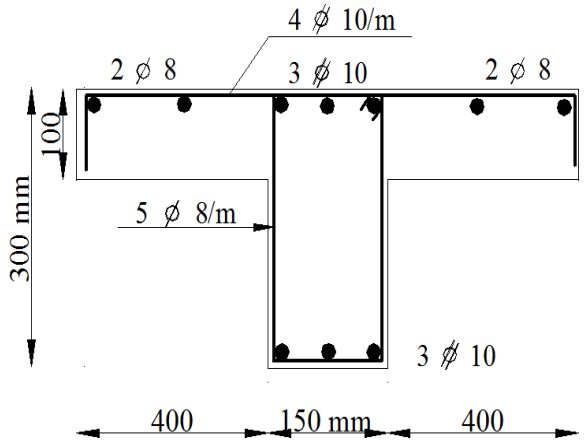

Figure 5 (b). Plan of specimen GIIID-2

Concrete Properties

All specimens were concreted at the same time with concrete coming from the same batch with a target 28-day specified strength of 25MPa. The Ordinary Portland cement (Type I) content of concrete was 350 kg/m^3 with a water-cement ratio (w/c) of 0.50. The nominal maximum size of aggregate size was 20mm and content of concrete was 1256kg/m^3 while, natural clean sand (fine aggregates) content was 628kg/m^3. In addition, to determine the compressive strength of concrete after 7 and 28 days from the pouring of concrete, 18 standard cube tests 150×150×150mm^3 were also cast; 9

concrete cubes were tested after 7 days and the remaining cubes were tested after 28 days. All specimens were casted from the same concrete mix for which the average compressive strength was 23.44MPa at 7 days, while at 28 days was equal to 29.76MPa.

Test setup and instrumentation details

The tests were carried out in a 100-ton universal testing machine. Each T-beam section was tested as a simply supported beam by using a vertical hydraulic jack. Linear varying displacement transducers (LVDTs) were installed at the mid-span of slab and beam to record the central deflections of the slab and the beam at different loading levels. Cracks were detected through visual observation during the testing of all specimens, as well as marking the propagation of cracks at each load increment. The cracking and ultimate loads were accurately recorded during each test.

3. RESULTS AND DISCUSSIONS FOR LOADING T-BEAM WITH UNIFORM DISTRIBUTED LOADS AT BOTH-EDGES OF SLAB

Crack pattern and failure mechanism

For Specimens GIM: Fig. 6 shows the cracks pattern for control specimen GIM-1 (t_{mis}/t_s = 20%). During testing of this specimen, the first visible crack was initiated in the border line between slab (flange) and beam (web) at load equal to 10kN on both sides of the beam. These cracks were started in the region of the maximum tensile stress in the slab. These cracks extended on the boundary between the slab and the beam along the entire length of the specimen. Then, by increasing the applied load, the cracks grow wider and deeper until the failure of the slab. The failure was flexural failure and the ultimate load was about 32kN.

For testing of the remaining specimens GIM-2, GIM-3 and GIM-4, it was observed that the cracks were initiated at one side of border line between slab (flange) and beam (web) spread along the length of specimen. These cracks were extended along the overall length of the specimens and occurred due to slabs maximum bending moment. The loads at the initial cracks were about 5kN, 4.5kN and 4kN for specimens GIM-2, GIM-3 and GIM-4, respectively. At the failure of these specimens, the width of the cracks was noticeably widened and highly propagated at the face of the intersection between slab and beam where the height of reinforcement in slab reduced. The specimens were failed when the applied loads reached about 25kN, 20.5kN and 18.5kN for specimens GIM-2, GIM-3 and GIM-4, respectively. It was noticed that; the specimens were suddenly failed. This may due to the misplacement of slab reinforcement, especially in specimens GIM-3 and GIM-4, where (t_{mis}/t_s) of these specimens were 60% and 80%, respectively. **Figs. 7, 8** and **9** show the photo of specimens GIM-2, GIM-3, and GIM-4, respectively after the failure.

Figure 6. Cracks pattern of specimen GIM-1

Figure 7. Cracks pattern of specimen GIM-2

Figure 8. Cracks pattern of specimen GIM-3

Figure 9. Cracks pattern of specimen GIM-4

For Specimens GIIA: The specimens GIIA-1 and GIIA-2 exhibited basically the same cracking pattern and final mode of failure in nature of loading. The failure of the specimens was flexural tensile failure in the slab at the interface lines between the slab and attached beam. Also, the cracks were started in the region where there was no reinforcing bars in the slab and propagated towards the loading points. The first crack was initiated at loads of about 7.5kN and 9kN for specimens GIIA-1 and GIIA-2, respectively. In case of specimen GIIA-1, horizontal cracks appeared in slab at early loading levels and inclined towards the loading lines, especially, were spread in the zones where there was no main reinforcement in the slab. This may be due to the improper rebar spacing of slab reinforcement. As the load was further increased, the crack became wider and extended at both sides of the beam on the overall length of specimen up to failure. The specimens GIIA-1 and GIIA-2 were failed at loads of about 28kN and 30.5kN, respectively. This may due to the existence of three reinforcing bars close to each other led to an increase in the efficiently of slab to loading effect over specimen GIIA-1. The unequal distribution of slab reinforcing steel in the negative moment zones resulted in improper slab resistance to the loads. The cracking patterns of tested specimens GIIA-1 and GIIA-2 at failure are shown in **Figs. 10** and **11**, respectively.

Figure 10. Cracks pattern of specimen GIIA-1

Figure 11. Cracks pattern of specimen GIIA-2

For Specimens GIIID: The cracks patterns for specimens GIIID-1 and GIIID-2 are depicted in **Figs. 12** and **13**, respectively. The first cracks were longitudinal flexural cracks in the vicinity of the tension zone within and near the maximum moment region at the connection of slab (web) with beam (flange) at a load of about 4.60kN and 7kN for specimens GIIID-1 and GIIID-2, respectively. These cracks were continued on the overall length of specimen.

For specimen GIIID-1, at higher loading stages, the rate of formation of new cracks significantly decreased. Moreover, the existing cracks grow wider, especially the initial formed cracks. The specimen failed at ultimate load of about 19kN in the region of maximum negative moment affecting on T-beam section. Before failure, diagonal crack was appeared and propagated toward the connection of the beam to the slab and continued in the slab in the direction of loading.

For the specimen GIIID-2, with the increase in load, cracks are appeared at the borderline between the beam and the slab. The width of the cracks was increased with the increase in the loading up to ultimate load at load of about 38kN. A crushing of the concrete in one corner of the specimen occurred when loading increased. This specimen exhibited a high resistance to the loads compared with specimens GIM-1 and GIIID-1 due to this slab is reinforced using a diameter of 10mm. It could be concluded from these results that an increase in the diameter of slab reinforcement while keeping reinforcement ratio constant, enhanced the behavior of T-beam to withstand the loads and increased the ductility of the T-beams. It also improves the efficiency of T-beam section under loading effect. It is preferred the minimum bar diameter for slab reinforcement is 10mm (high-tensile steel) because the 8mm and 6mm diameters reinforcement (mild steel) were found to be weak in resisting the loads.

Figure 12. Cracks pattern of specimen GIIID-1

Figure 13. Cracks pattern of specimen GIIID-2

Load-Deflection behavior at the edge of slab for tested specimens

The total applied load, P was plotted against the vertical deflection, Δ measured at the edge of slab in mid-span for all tested specimens. The cracking load P_{cr}, ultimate load P_u, toughness and type of failure for all tested specimens are shown in **Table 2**.

Table 2. Summary of the results for loading T-beam with uniform distributed loads atnboth-edges of slab

Specimen Notation	Cracking Load (Pcr)(kN)	Ultimate Load (Pu) (kN)	Pcr Pu	Pu (Control)	Toughness (kN.mm)	Toughness Ratio	Failure Type
GIM-1 (Control)	10	32	0.31	1.0	981.21	100%	Flexural cracking at both-sides of slab
GIM-2	5	25	0.20	0.781	701.81	71%	Flexural cracking at one side of slab at border line among slab and beam
GIM-3	4.5	20.50	0.22	0.640	589.82	60%	
GIM-4	4	18.50	0.32	0.578	496.95	50%	
GIIA-1	7.5	28	0.24	0.875	828.08	84%	Flexural cracking at both-sides of slab
GIIA-2	9	30.5	0.42	0.953	973.09	99%	
GIIID-1	4.6	19	0.24	0.593	606.64	61%	Flexural cracking at both-sides of slab
GIIID-2	7	38	0.18	1.187	1412.7	143%	

For Specimens GIM: it was noticed that; the tested specimens indicated linear behavior before cracking. After cracking, specimen's stiffness were decreased as the load increased. For specimens GIM-2, GIM-3 and GIM-4, lower values of the ultimate load and deflection were noticed compared with the control specimen GIM-1. The initial crack load for the specimens GIM- 1, GIM-2, GIM-3 and GIM-4 was 10kN, 5kN, 4.5kN and 4kN, respectively. While, load carrying capacity of these specimens was about 32kN, 25kN, 20.5kN and 18.5kN, respectively. At the same time, the maximum deflections, Δu at failure for specimens GIM-1, GIM-2, GIM-3 and GIM-4 was 33mm, 31mm, 32mm and 32mm,respectively. The first crack was initiated at the load 31.25%, 20%, 21.95% and 21.60% from the ultimate load for specimens GIM-1, GIM-2, GIM-3 and GIM- 4, respectively. The area under the load-deflection relationship up to failure is called toughness, as shown in **Table 2**. **Fig. 14** shows load-deflection relationships for the tested specimens of group GIM.

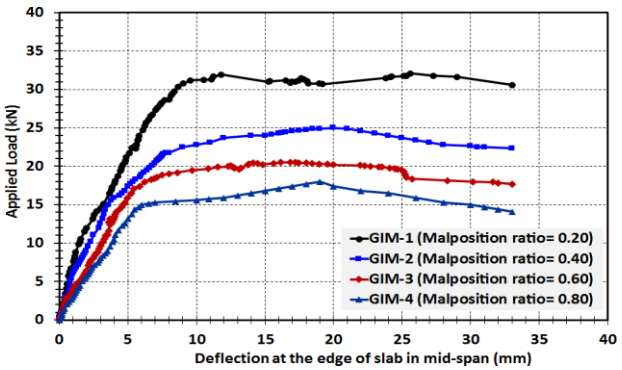

Figure 14. Comparison between the tested specimens of group GIM

It was obvious that; the control specimen GIM-1 was the highest in resistance of the loads compared to the remaining specimens of this group GIM. Increasing the malposition ratio (tmis/ts) from 20% to 40% decreases the ultimate load with about 21.87%. When the malposition ratio (tmis/ts) reached to 60%, the decrease in the ultimate load reached to about 35.93%. When the malposition ratio (tmis/ts) reached to 80%, the decrease in the ultimate load reached to about 42.18%. Thus, it could be concluded from the previous results that, as the malposition ratio (tmis/ts) increased, the ultimate load decreased and the corresponding slab deflection increased. This may attribute to the fact that, as the malposition ratio (tmis/ts), increase, the effective depth of the slab decrease and consequently flexural resistance decrease and slab deflection increase.

Finally, it could be said that; a misplaced position of the reinforcement can be caused by deficient support of the reinforcement during

the implementation and the pouring of the concrete. A lower place of the reinforcement leads to a lower bending moment capacity of the slab and can also lead to a brittle behavior in case of collapse.

For Specimens GIIA: The load-deflection relationships of the two specimens GIIA-1 and GIIA-2 were compared with that of the control specimen GIM-1, as shown in **Fig. 15**.

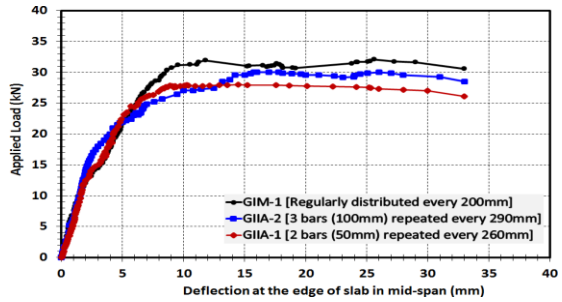

Figure 15. Load–deflection relationships for specimens GIIA

It was clear from the aforementioned comparison that; all specimens GIM-1, GIIA-1 and GIIA-2 behaved in a same trend at the beginning of the load and illustrated linear load-deflection behavior up to first crack. The first cracking load in specimens GIM-1, GIIA-1 and GIIA-2 was started at load 10kN, 7.5kN and 9kN, with percentage 31%, 24.5% and 29.5% from the load carrying capacity for specimens GIM-1, GIIA-1 and GIIA-2, respectively. Also, it could be noted that; there was a pronounced difference between the three specimens in terms of load and deflection for all load increment up to the ultimate loads. After the ultimate load, significant differences were noted in the load-deflection curves of the three specimens. The ultimate load for GIM-1, GIIA-1 and GIIA-2 was 32kN, 28kN and 30.5kN, respectively. However, the control specimen GIM-1 recorded an increase of 12.5% and 4.68% in the ultimate load over specimens GIIA-1 and GIIA-2, respectively.

It can be concluded that; the irregularity of the reinforcing steel in concrete slabs affected the load carrying capacity of these slabs. As the load carrying capacity of the slab reduced when the spacing between the reinforcing bars increased. Meanwhile, irregularity of main steel creates a sort of non-uniform stress distribution over the section and accelerated the failure.

For Specimens GIIID: The load-deflection relationships of specimens GIM-1, GIIID-1 and GIIID-2 are plotted in **Fig. 16**.

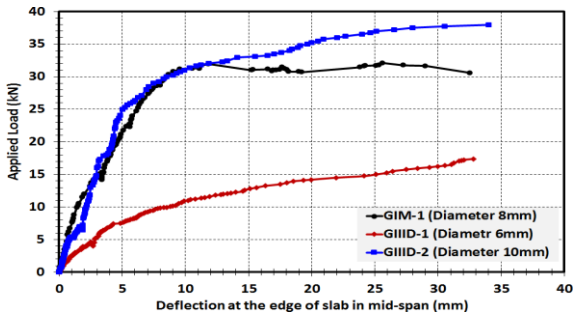

Figure 16. Comparison between the tested specimens GIII

The comparison of group GIIID showed that the use of 10mm diameter in the reinforcement of the slab exhibited high resistance to loads while on the contrary, the 6mm diameter reinforcement offered a weak resistance to the loads affecting the slab. The ultimate loads for specimens GIM-1, GIIID-1 and GIIID-2 were about 32kN, 19kN and 38kN and deflection values at failure were 33mm, 33mm and 34mm, respectively. Specimen GIIID-2 experienced higher deflection than that of specimen GIM-1 specimen due to high load carrying capacity. The load of specimens GIIID-1 and GIIID-2 was about 40.70% and 18.75 % compared to specimen GIM-1, taking into consideration that the yield stress of the steel with diameter lower than or equal to 8mm was 240N/mm^2 (mild steel and smooth bars) while, for steel with diameter 10mm (deformed bars) the yield stress was about 360N/mm^2 (high-tensile steel).

Load-deflection responses for specimens GIM-

1 and GIIID-2 showed approximately the same trend and no significant difference was observed at low loading level, while the third specimen GIIID-1 exhibited a significant difference in the deflection from the beginning of loading. After the initial flexural crack between the slab and beam, large difference between specimens GIM-1 and GIIID-2 response was noted. The first crack load represents about 31%, 24.2% and 18.4% of the ultimate load for specimens GIM-1, GIIID-1 and GIIID-2, respectively. The flexural crack resulted in a decrease in the instantaneous stiffness of the specimen. After the formation of the flexural cracking, the stiffness decreased more rapidly and up to failure.

From the test results of group GIII, it is concluded that with the increase in bar diameter of slab reinforcement, stiffness of slab increases and subsequently the resistance of the load are high. Diameter 10mm had corrugated surface that increased the bond and reduced bond slippage of the bar in the concrete. Furthermore, diameter 10mm had high yield strength. Instead, normal mild steel bars had smooth surface and low strength which reduced their bond strength with concrete.

Load-Deflection behavior at mid-span of the attached beam

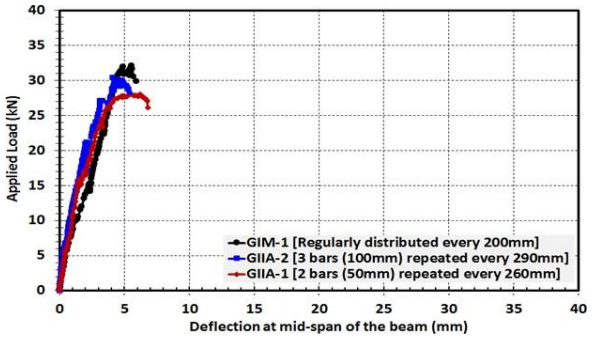

Figure 17. shows load-deflection relationship at mid-span of the attached beams for group GIM.

It is apparent that the shape of the load-deflection curves in the elastic region before cracking is the same for the all specimens. However, it appears that after cracking, both specimens GIM-1 and GIM-2 produced higher values of deflection than specimens GIM-3 and GIM-4 for the same level of loading. The maximum deflection of specimens GIM-1, GIM-2, GIM-3, and GIM-4 was 5.9mm, 6.7mm, 7.55mm, and 6.3mm, respectively at the failure load. It can be said that the ill effect from the malposition of slab reinforcement is more serious on the behavior of slab and the attached beam than the correct place for reinforcing steel for the slab.

The load-deflection curves for specimens of group GIIA are shown in **Fig. 18**. There is no significant difference between three specimens in the values of deflection, especially at the beginning of loading before the initiation of cracks. The maximum deflection for the specimens GIM-1, GIIA-1 and GIIA-2 at the failure load was 5.90mm, 6.80mm, and 5.75mm, respectively.

It is evident that the irregularity of the reinforcement of slab does not have any significant effect on the efficiency of a concrete beam connected with the slab. Furthermore, the beam attached to slab was not significantly affected by the irregularity of the shape of slab reinforcement.

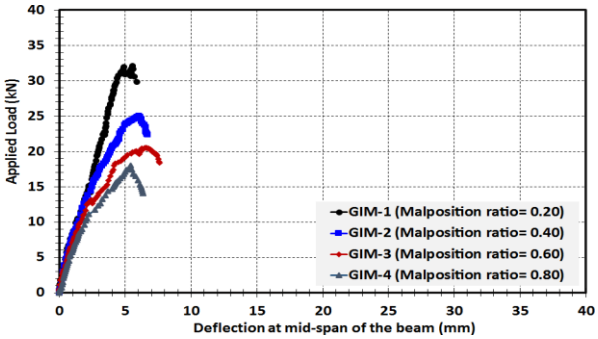

Figure 18. Comparison between the tested specimens of group GI

It was found that the use of 10mm diameter in reinforcing the slab in T-section significantly

improved the flexural behavior of the slab to resist the load. Thus, the behavior of the beam connected to the slab.

improved to withstand the loads. Also, there is no clear difference between the behavior of specimens GIM-1 and GIIID-2 with slab reinforcement with diameters 8mm and 10mm in load- deflection values. The maximum deflection value for the beam at the failure was 5.9mm, 8.75mm and 10.25mm for specimens GIM-1, GIIID-1, and GIIID-2, respectively. Specimen GIIID-2 demonstrated higher deflection than specimen GIM-1 and GIIID-1 where this specimen reinforced the slab with a diameter of 10mm, showed the beam connected to the slab a high resistance to loads. Therefore, it is preferable to use 10mm or higher diameter in reinforcing the slabs.

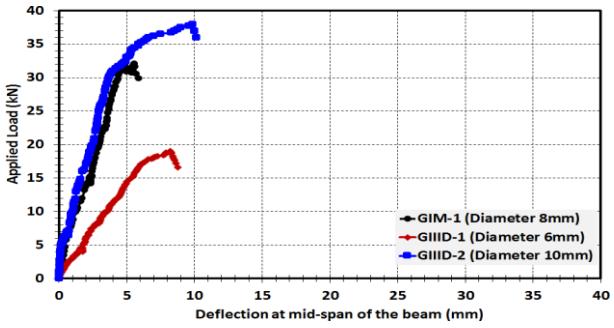

Figure 19. Comparison between the tested specimens of group GIII

4. CONCLUSIONS

Based on the experimental test results obtained in this investigation, the following conclusions can be drawn:

1. The malposition ratio increased, the ultimate load decreased and the slab deflection increased. If this ratio increased from 20% to 40%, 60%, and 80% results in reduction of the ultimate load by about 21.87%, 35.93% and 42.18% respectively. This may attribute to the fact that, as the malposition ratio increased, the effective depth of the slab decreased and consequently flexural resistance decreased and slab deflection increased.
2. A misplaced position of the reinforcement can be caused by deficient support of the reinforcement during the implementation and the pouring of the concrete. A lower place of the reinforcement leads to a lower capacity of the slab and can also lead to a brittle behavior in case of collapse.
3. The irregularity of the reinforcing bars in concrete slab affected the load carrying capacity of T-beam. The increases in the spacing of reinforcing bars decreased the ultimate load, where the specimen with well-arranged distribution of reinforcement (control specimen GIM-1) recorded an increase of 4.70% and 12.50% in the ultimate load over specimens GIIA-1 and GIIA- 2, respectively (irregular arrangement specimens).
4. Well-arranged distribution of reinforcement improves the ductile behavior of slab and reduced value of deflections at failure. Meanwhile, irregularity of main steel created a sort of non- uniform load distribution over the section and accelerated the failure.
5. Using reinforcing steel bars with diameters higher than 8mm in the reinforcement helped the slab to withstand more loads and delayed the occurrence of failure of the slab and connected beam.
6. The increasing of the diameter of slab reinforcement while keeping reinforcement ratio constant enhanced the behavior of T-beam to withstand the loads. Specimen with diameter 10mm showed 18.75% increase in ultimate load compared to specimen with diameter 8mm (smooth surface) while specimen with diameter 6mm decreased 59.30% lower than the specimen with diameter 8mm.

Acknowledgements

I would like to thank all the people who contributed in some way to the work described in this paper. The authors gratefully acknowledge their generous support.

Conflict of interest

The authors declare no conflicts of interest.

Funding

No funding was received for this research.

REFERENCES

[1] Neha.V. Bagdiya and Shruti Wadalkar. Review Paper on Construction Defects. Journal of Mechanical and Civil Engineering. 2015, Vol. 12 (2), PP: 88-91.

[2] Egyptian code of practice for design and construction of reinforced concrete structures (ECCS203-2007). Housing and Building Research Center, Giza, Egypt.

[3] ECP203-2007, Egyptian Code of the Design and Construction ofReinforced Concrete Structures, Housing and Building NationalResearch Center, Egypt.

[4] *(PDF) Experimental evaluation of the common defects in the execution of reinforced concrete beams under flexural loading*. Available from: https://www.researchgate.net/publication/257681416_Experimental_evaluation_of_the_common_defects_in_the_execution_of_reinforced_concrete_beams_under_flexural_loading [accessed Apr 29 2022].

[5] ACI Committee Report 224.1R-93. Causes, Evaluation and Repair of cracks in Concrete Structures. American Concrete Institute Journal, September (1993) 1-22.

[6] Elrakib, T. and Arafa, A. Experimental Evaluation of the Common Defects in the Execution of Reinforced Concrete Beams under Flexural Loading. HBRC Journal. 2012, Vol. 8, PP: 47-57.

[7] Afunanya, J.E. Assessment of Construction Errors in Reinforced Concrete Beams. International Journal of Civil and Structural Engineering. 2015, Vol. 6 (1), PP: 105-118.

[8] A.Kh. Baiburin. Errors, Defects and Safety Control at Construction Stage. Procedia Engineering. 2017, Vol. 206: PP: 807–813.

[9] Ribas González C. R., Fernández Ruiz M. Influence of flanges on the shear-carrying capacity of reinforced concrete beams without web reinforcement. Structural concrete journal. 2017, Vol. 18, PP: 720-732.

[10] Zhang Yannian, Xie Jun and Wang Liu. Experimental Study on RC T-Section Beams Strengthened with Bottom Steel Plates. Jordan Journal of Civil Engineering. 2018, Vol. 12, No. 3, PP: 502-515.

[11] P. Eswaramoorthi, P. Sachin Prabhu and P. Magudeaswaran. Experimental Study of Reinforced Concrete Continuous Rectangular and Flanged Beams at Support Region. International Journal of Civil Engineering and Technology. 2017, Vol. 8, PP: 706–713.

[12] Ibrahim G. Shaaban, Messaoud Saidani, Muhd Fadhil Nuruddin, Ahmad B. Malkawi and Tarek S. Mustafa. Serviceability behavior of Normal Strength Concrete and High Strength Concrete T-beams. European Journal of Materials Science and Engineering. 2017, Vol. 2, Issue 4, PP: 99-110.

[13] Rendy Thamrin, Jafril Tanjung, Riza Aryanti, Oscar Fitrah Nur and Azmu Devinus. Shear strength of reinforced

concrete T-beams without stirrups. Journal of Engineering Science and Technology. 2016, Vol. 11, No. 4, PP: 548 – 562.

[14] Amr H. Zaher, Wael M Montaser, and Ahmed K Elshenawy. Shear Behavior of Light Weight Concrete T –Beams. International Journal of Emerging Technology and Advanced Engineering. 2015, Vol. 5, Issue 12. PP: 243-252.

[15] Riadh Al-Mahaidi, Geoff Taplin, and Craig Giaccio. Experimental study on the effect of flange geometry on the shear strength of reinforced concrete T-beams subjected to concentrated loads. Canadian Journal of Civil Engineering. 2011, Vol. 29, PP: 911–918.

[16] Dhia B. Ghailan. T-Beam Behavior in Flexure with Different Layers of Concrete in Web and Flange. Kufa Journal of Engineering. 2010, Vol. 2, PP: 53-61.

[17] Withit Pansuk and Yasuhiko Sato. Shear Mechanism of Reinforced Concrete T-Beams with Stirrup. Journal of Advanced Concrete Technology. 2007, Vol. 5, No. 3, PP: 395-408.

[18] Marta Słowik. The analysis of failure in concrete and reinforced concrete T-beams with different reinforcement ratio. Archive of Applied Mechanics. 2019, Vol. 89, PP: 885– 895.

[19] Ribas González C. R., Fernández Ruiz M. Influence of flanges on the shear-carrying capacity of reinforced concrete beams without web reinforcement. Structural Concrete Journal. 2017, Vol. 18, PP: 720-732.

[20] Hesham A. Amna and Wael M. Monstaser. Shear behavior of reinforced lightweight concrete T-beams. Life Science Journal. 2019, Vol. 16(8). PP: 11-27.

[21] Ofonime A. Harry and Ndifreke E. Udoh. Effect of Flange Width on Flexural Behavior of Reinforced Concrete T-Beam. Civil and Environmental Research Journal. 2016, Vol. 8, No.8, PP: 97-103.

[22] Zhuangcheng Fang, Haibo Jiang, Airong Liu, Jiahui Feng and Yuanhang Chen. Horizontal Shear Behaviors of Normal Weight and Lightweight Concrete Composite T- Beams. International Journal of Concrete Structures and Materials. (2018) 12:55, PP: 1-21.